



# HHS Public Access

Author manuscript

*Footwear Sci.* Author manuscript; available in PMC 2023 September 29.

Published in final edited form as:

*Footwear Sci.* 2022 ; 14(3): 219–228. doi:10.1080/19424280.2022.2124319.

## Shoe Tread Wear Occurs Primarily during Early Stance and Precedes the Peak Required Coefficient of Friction

Rosh Bharthi,

Joseph R. Sukinik,

Sarah L. Hemler,

Kurt E. Beschorner\*

Department of Bioengineering, University of Pittsburgh, 301 Schenley Place, 4420 Bayard St., Pittsburgh, PA 15213, United States

### Abstract

Worn shoes contribute to injuries caused by slip-and-fall accidents. The peak required coefficient of friction (RCOF) has been associated with tread wear rate. However, the temporal relationship between RCOF and shoe wear is unknown. The purpose of this study was to determine whether the contact region at the time of peak RCOF is consistent with the region of shoe wear. The shoe contact region at peak RCOF was imaged by frustrated total internal reflection. Images of worn tread after months of use were captured. The worn tread region was more posterior than the contact region at RCOF and did not correlate with the contact region at the time of RCOF. The contact regions observed during earlier stance (within 83 ms of heel contact) were more consistent with the worn region, suggesting that RCOF may not directly cause tread wear. These results serve to motivate future studies to identify early-stance gait parameters associated with tread wear development.

### Keywords

Slip-and-fall; Shoe wear; Tread wear; Required coefficient of friction (RCOF); Frustrated total internal reflection (FTIR)

### Introduction

Slip-and-fall accidents are among the most common form of workplace injury (National Institute for Occupational Safety and Health, 2020). In 2019, 305,000 workers experienced nonfatal injuries from falls, slips, and trips, 87,000 of whom were injured from same-level slip and fall events (U.S. Department of Labor- Bureau of Labor Statistics, 2020a, 2020b). In response to this problem, a need exists for the research community to develop solutions that reduce slip risk and prevent occupational falls.

---

\*Corresponding author: Kurt E. Beschorner, PhD, Schenley Place #306, 4420 Bayard St., Pittsburgh, PA 15213 beschorne@pitt.edu, 412 - 624 - 7577.

Declarations of interest:

The authors have no financial conflicts of interest to disclose.

Shoe wear is one important factor that influences the likelihood of a slip accident (Bell et al., 2019; Verma et al., 2011; Verma et al., 2014). For liquid-contaminated surfaces, increased tread wear eliminates tread channels and deteriorates the under-shoe fluid drainage capacity (Beschoner et al., 2014; Hemler et al., 2019). The tread wear results in increased fluid pressure between the shoe and floor, decreased friction, and a higher slip risk (Sundaram et al., 2020).

Accurately characterizing shoe wear is relevant to assessing the slip risk of shoes. The slip risk associated with shoes is commonly assessed by measuring the coefficient of friction between the shoe and a floor surface with a liquid contaminant (Beschoner et al., 2019; Iraqi et al., 2020; Jakobsen et al., 2022; Wilson, 1990). One challenge associated with this characterization is that the friction performance of footwear changes as it becomes worn (Grönqvist, 1995; Hemler et al., 2020; Hemler et al., 2022). To assess durable footwear performance, methods of simulating wear have been developed so that shoe performance in a worn condition can be characterized (Heeluxe Inc., 2021; Hemler, et al., 2019; Satra Technology, 2022). However, a lack of current evidence exists regarding whether these devices simulate the salient aspects of gait-induced wear to reflect the wear patterns that occur naturally. Therefore, additional research is needed to capture the location of shoe wear patterns and the gait phases that correspond with this location.

Given that worn shoe treads can lead to increased slip risk, predicting wear patterns and understanding tread wear mechanisms are important. Research to predict wear and understand the underlying mechanisms of wear are emerging. Previous research has applied the empirical relationship of the Archard wear equation that relates the wear rate to the amount of normal load or contact pressure (Moghaddam et al., 2019). This data suggested that the contact regions predicted by finite element analysis were associated with the worn region that forms in response to abrasion experiments (Moghaddam et al., 2019). The topography of the shoe surface similarly suggests that abrasion could be an important wear mechanism (Hale et al., 2021). Another study that assessed natural wear in the work environment found that shear forces during walking can predict wear rate suggesting that shear forces are a relevant contributing factor (Hemler et al., 2021). Thus, shoe wear is potentially dependent on multiple kinetic measures including the normal and shear forces.

A common metric for characterizing the shear forces during walking is the required coefficient of friction (RCOF) (Hanson et al., 1999; Hemler et al., 2021). RCOF has traditionally been used to characterize an individual's risk of slipping and has more recently been found to be associated with shoe wear (Beschoner et al., 2016; Hemler et al., 2021; Sundaram et al., 2020). RCOF is defined as the ratio of shear force to normal force during gait (Hanson et al., 1999). In addition, the determination of RCOF also includes temporal considerations. Six local peaks in the time-series of shear force to normal force ratio can be observed during stance (Perkins, 1978). Of these peaks, the third or fourth peak is commonly used to characterize forward slip risk (Chang et al., 2011; Perkins, 1978). Because peak RCOF is correlated with wear rate (Hemler et al., 2021), we hypothesized that the instance in gait when peak RCOF is achieved is related to tread wear. That is, the portion of the heel contacting the ground at peak RCOF would align with the worn tread region after months of use. Confirmation of this hypothesis would indicate that the

contact region at the time of RCOF is most susceptible to wear and should be prioritized for wear-tolerant designs. Identifying the time point in gait when wear occurs could also allow for better predictive models and other design interventions to reduce tread wear or predict shoe replacement needs.

The purpose of the study was to determine the time in stance that is most relevant to shoe wear. Specifically, this study aims to assess the congruence between the contact area at RCOF and the worn region after prolonged use.

## Methods:

This study included a biomechanics component where the participants' gait was measured and a longitudinal component where participants wore shoes at work, while the wear pattern was tracked. Portions of this data set have been previously described including the changes in friction performance shoes due to shoe tread wear (Beschoner et al., 2020; Hemler et al., 2020; Hemler et al., 2022) and the relationship between wear rate and RCOF (Hemler et al., 2021). The present study uses imaging of the shoe contact region from the gait analysis to characterize the time of stance most relevant to shoe wear, which has not been previously reported.

## Participants

Eight participants (6 male and 2 female; age:  $37\pm 13$  years; height:  $173\pm 6$  cm; mass:  $173\pm 6$  kg) were selected for the analysis from a cohort of fourteen participants from a previous study (Hemler et al., 2021). Participants were each given two of the three slip-resistant, rubber (manufacturers did not specify the exact material) outsole shoe designs that were part of this study (Shoe A,  $n=5$ ; Shoe B,  $n=4$ ; Shoe C,  $n=3$ ). The brand, tread shape, dimensions, tread depth, hardness, and heel height for the shoes are included in Table 1. Inclusion criteria for participants consisted of frequently wearing treaded shoes, a working environment where the flooring consisted of manmade surfaces for more than 75% of their walking time, and where participants were on their feet for at least 4 hours in each day. Exclusion criteria included neurological problems, musculoskeletal history/disorders, osteoporosis, or arthritis. Data from the cohort of 14 qualified for this secondary analysis if the heel landed in the center of a video camera's field of view during the gait trials ( $n=6$  excluded). Participants provide informed consent and the project was approved by the University of Pittsburgh Institutional Review Board.

## Gait Assessment

Participants completed gait trials during which they walked over a transparent frustrated total internal reflection (FTIR) plate and a force plate (Bertec 4060A, Columbus, OH) (Needham & Sharp, 2016). A camera (120 fps sampling rate) beneath the FTIR plate recorded a video of the participant shoe's contact regions during the stance. Force data was captured at 1080 Hz. Three-dimensional force values during stance were collected from ten force plate hits for each participant, with five hits per foot.

## Wear at work

After the gait assessment, participants completed a longitudinal study to track shoe wear. The participants wore the shoes in their normal workplace for a period of at least one month and up to 12 months. Their workplaces were primarily indoors and consisted of the following industries: trade, transportation & utilities, manufacturing, leisure and hospitality, and education and health services. Participants alternated between the two shoe designs each month. These shoes were primarily used in the participants' occupational settings although they may have been worn in other settings. After each month of the wear periods, pictures were taken of the worn heel portion of the sole so the worn region could be characterized. The wear of both left and right shoes was characterized.

## Data Processing

A custom data processing code (Matlab, Mathworks, Natick, MA, USA) was created to obtain the time of peak RCOF during stance. Heel contact was defined as the instance when the normal force exceeded 10 N. Force data during the first 200 ms after heel contact were used for obtaining the peak RCOF time point. A vector sum of shear forces was calculated for each time point, and a ratio of the vector sum and the corresponding normal force was calculated to obtain this ratio over time (Beschorner et al., 2016; Chang et al., 2011; Hemler et al., 2021; Sundaram et al., 2020). Only shear forces in the braking direction (i.e., anterior/posterior component of force was opposite the walking direction) during stance were candidates for selecting the peak RCOF. Peak RCOF was defined as the local maximum of the RCOF values when the normal force exceeded 100 N. Time-series plots of the ratio of shear to normal force were reviewed to ensure that the time of RCOF corresponded to either peak 3 or 4 identified in Perkins (1978). In cases where the algorithm selected the wrong peak, the correct peak was manually selected. The time corresponding to peak RCOF was recorded.

A custom image analysis code (Matlab, Mathworks, Natick, MA, USA) was created to determine the centroids of the contact regions from the FTIR videos. Each image from the video was converted from color to 8-bit grayscale. Next, the heel region was cropped using a series of selected points that were fitted with a spline function (Cazzaniga, 2021). In the resulting cropped image, the contact region was distinguished by bright pixels and the non-contact region was characterized by dim pixels. A researcher selected eight pixels from the contact region to calibrate the brightness thresholds used to identify the contact region. In particular, the user selected four bright pixels and four dim pixels from the perceived contact region. Using the brightness values of the 8 selected pixels, pixels within the cropped region were determined to be in contact if their brightness was within a range from 1.5 standard deviations below the mean value to 2 standard deviations above the mean value. The center (average) position of all pixels in contact was identified. The center was referenced to a local coordinate system with an origin of the posterior-most point of the shoe, a y-axis along the length of the shoe (anterior), and a positive x-axis oriented laterally. Frames of video data corresponding to RCOF and the first 83 ms after heel contact were analyzed. The analysis considering the first 83 ms was conducted after the RCOF analysis revealed that contact centroid during the RCOF time was anterior to the wear centroid (see Results section). Subsequently, the FTIR videos were checked and it was determined that

the contact centroid passed the wear centroid within 83 ms of heel contact for all of the participants in this study.

A custom image analysis code (MATLAB) was created to find the centroids for the wear regions. After loading the image of the worn heel tread, a spline function was fitted to points that cropped the image to only include the visibly worn treads. The centroid of the cropped wear region was determined. Similar to the processing of the FTIR images, the coordinates were referenced to the same local coordinate system described previously.

Because the analysis relied on obtaining valid FTIR plate videos where the heel strike was in-frame and centered, not every participant's right and left shoe was included in the analysis. Of the 12 participant-and-shoe combinations with good FTIR plate videos, 9 had both right and left shoes analyzed, 2 had only right shoes, and 1 had only the left shoe. Thus, 21 shoes were used in the analysis.

The FTIR data and worn region data were analyzed to determine: 1) the association between contact region at RCOF and the worn region; 2) the time point that led to the best agreement between contact region at RCOF and the worn region; 3) the agreement between the early-stance contact region and the worn region. Robust regression analysis was performed between the contact centroid at RCOF and the worn region centroid. For these correlation analyses, the medial-lateral and anterior-posterior analyses were analyzed separately. In response to results suggesting that wear occurs earlier in the gait cycle than the RCOF peak (described in the Results section), additional analyses were performed to identify the time of contact that best aligned with wear. The resultant distance between the worn region centroid and the contact region centroid was calculated for each frame of data. The minimum distance between the contact and wear centroids was calculated for each shoe to represent the time point where the contact region most closely resembled the worn region. Robust regression (separate analyses for anterior/posterior and medial/lateral directions) between the contact centroid at this time and the wear centroid were performed to confirm agreement between this selected point and the wear region (MATLAB R2018a, Mathworks, Natick, MA). Statistical analyses were performed with an alpha of 0.05 and the data set was sensitive to capture correlation coefficients greater than 0.54 (assuming a power of 80%). Lastly, each tread lug (individual tread projection) was compared between the worn shoe and the FTIR image associated with the closest point to determine if the same tread was present in both the FTIR image and the worn region, only in the FTIR image, or only in the worn region.

## Results:

Across all participants, peak RCOF was achieved  $114 \pm 16$  ms (range: 90 – 146 ms) after heel contact. There was no correlation between the center of the contact region at the time of RCOF and the center of the wear region (Figure 1). This finding was also visually confirmed when comparing the FTIR and worn shoe images (Figure 2, A and B). Across all shoe types, the contact region at peak RCOF was 0 mm, standard deviation (s.d.): 4 mm (range: -10 – 7 mm) medial from the shoe's midline and 65 mm, s.d. 13 mm (range: 46 – 96 mm) anterior to the heel edge. The wear region was 13 mm, s.d. 11 mm (range: -11 – 29 mm) lateral

from the shoe's midline and 31 mm, s.d. 10 mm (range: 6 – 47 mm) anterior to the heel edge. The adjusted  $R^2$  value for the correlation between the FTIR image centroid and worn region centroid was 0.00 ( $F_{1,19}=0.0$ ,  $p=0.852$ ) for the mediolateral axis coordinates and 0.00 ( $F_{1,19}=0.4$ ,  $p=0.532$ ) for the anterior-posterior axis coordinates (Figure 1).

The timepoints when the contact region center was closest to the worn region center revealed that the contact region during early stance was consistent with the worn region. Across all shoe types, the contact region for the image best aligning with the worn region was 4 mm, s.d. 6.2 mm (range: -4 – 15 mm) lateral from the shoe's midline and 29 mm, s.d. 14 mm (range: 4 – 48 mm) anterior to the heel edge. As mentioned previously, the wear region was 13 mm, s.d. 11 mm (range: -11 – 29 mm) lateral from the shoe's midline and 30 mm, s.d. 10 mm (range: 6 – 47 mm) anterior to the heel edge. The adjusted  $R^2$  value for the correlation between the selected FTIR image centroid and worn region centroid was 0.417 ( $F_{1,19}=15.3$ ,  $p<0.001$ ) for the mediolateral axis coordinates and 0.744 ( $F_{1,19}=59.2$ ,  $p<0.001$ ) for the anterior-posterior axis coordinates (Figure 3). Therefore, the selected frame was more closely associated to the worn region in the anterior-posterior direction than the medial-lateral direction. The median timepoint when the contact region was closest to the corresponding wear region was 67 ms after heel contact, the interquartile range was from 33 ms to 75 ms, and the range was from 17 ms to 83 ms (Figure 4).

The FTIR image captured some but not all treads that display wear (Figure 5). Furthermore, a high number of treads were in contact as measured in the FTIR image but did not lead to wear. The percentage of tread that were both in contact with the ground and were worn relative to all tread in the analysis ranged from 25–40.5% across shoe types. The percentage of tread that was in contact with the ground but not worn ranged from 35–62.9%, and the percentage of tread that was only worn but not in contact with the ground ranged from 12.1–31.3%. Shoe A exhibited the largest percentage of tread that were both in contact with the ground and worn where Shoe C showed the smallest percentage of tread that were in contact with the ground and worn.

## Discussion:

Based on the results of our study, the contact region at the time of RCOF did not predict the location of shoe wear. At the moment of peak RCOF, the region in contact with the ground was, on average, more anterior and medial compared to the worn region. The worn region was more consistent with the contact region earlier in stance (between 17 and 83 ms). The histogram of the contact time corresponding to the worn region (Figure 4) shows a potential bimodal distribution. It was noted that the contact region closest to the worn region either occurred near 25.0 ms (range: 17 – 42 ms) or 70 ms (range: 58 – 83 ms). These time points occurred well before RCOF was achieved, suggesting that wear likely occurs earlier in stance than peak RCOF. Importantly, the congruence between the contact regions and the worn region were not particularly high (Figure 5) suggesting that a single frame of contact data may be insufficient to predict wear. In addition, the analysis of the treads which were in contact with the ground and developed wear (Figure 5) suggest that contact is not a sufficient criterion for wear and that other factors may also be relevant.



Previous studies have shown that RCOF can predict slip risk for dry, level walking applications and is correlated with tread wear rate (Beschoner et al., 2016; Hemler et al., 2021). Based on this study's findings, the contact region at peak RCOF is anterior to the shoe wear region, suggesting that shoe wear is not caused by peak RCOF. This finding may suggest that RCOF is a marker but non-causal factor related to wear. It is possible that the under-shoe conditions (e.g., higher shear forces) at RCOF are representative of the under-shoe conditions earlier in stance when the wear occurs, which may explain the previously-reported correlation between RCOF and wear rate (Hemler et al., 2021).

The results of this study may indicate the potential for two mechanisms contributing to shoe wear. The bimodal nature of the time where worn region and contact best aligned may suggest multiple wear mechanism. For example, wear associated with early contact may be due to abrasion that occurs when the shoe strikes the floor during heel motion (i.e., scuffing). This would be consistent with wear associated with Archard's wear equation and that was simulated in some prior accelerated wear protocols (Hemler, et al., 2019; Moghaddam et al., 2019). Wear occurring from 50–83 ms occurs while the shoe is stationary and under kinetic shear (Cham & Redfern, 2002) suggesting that wear can also be caused by friction loading (Hemler et al., 2021).

Some limitations of the study should be acknowledged. A key challenge in assessing the relationship between shoe wear and gait biomechanics is that understanding of the mechanisms of shoe wear is emerging. Multiple mechanisms have been proposed including abrasive wear and wear from fatigue failure, which are expected to be dependent on different biomechanical aspects of gait. For example, abrasive wear is expected to be dependent on contact pressures and sliding distance during each step, while fatigue failure wear are expected to be dependent on the shear forces during gait (Hemler et al., 2021; Mars & Fatemi, 2002; Moghaddam et al., 2019; Moore, 1972). Improved understanding of these mechanisms is likely to enable the development of wear simulation devices that better reflect natural wear patterns. Contact data were analyzed for their correlation with the worn region in the present study. This analysis provided a key insight that wear is likely to occur early in stance (within the first 83 ms). Thus, devices that simulate wear should prioritize simulating shoe contact dynamics during early stance to generate more realistic wear patterns. However, wear likely occurs over a range of time during stance and may not be adequately captured by a single frame. Future studies may aim to integrate contact across multiple images to identify the time periods that are most relevant to wear. A key assumption was that wear radiates evenly from some center point and that the centroid would be independent of the level of wear. This effect can be qualitatively observed in the results by Moghaddam et al. (2019). However, this assumption has not been robustly tested. Thus, it is possible that using the area centroid from a 2D area does not perfectly align with volumetric centroid of the worn tread material. Lastly, gait patterns captured in the lab may not have reflected typical walking or the variability of walking occurring in workplace conditions. This variation could explain the difference in contact regions during stance and the wear regions over time.

The contact region at peak RCOF during stance is incongruent with the tread wear region after months of wear. Contact regions at earlier time points within 83 ms of heel contact

align more congruently with the locations of tread wear. Furthermore, the time points when contact region was closest to the region of shoe wear were bimodal. To further understand the mechanisms of tread wear during stance, future studies may seek to explore whether multiple wear mechanisms are responsible for wear and whether metrics that include kinetics and multiple time points are better able to predict the wear region.

## Acknowledgements:

This study was funded by grants from the National Institute for Occupational Safety & Health (NIOSH R01 OH010940), the National Science Foundation (NSF GRFP 1747452), and the National Center for Research Resources (NCRR S10RR027102).

## References:

- Bell JL, Collins JW, & Chiou S (2019). Effectiveness of a no-cost-to-workers, slip-resistant footwear program for reducing slipping-related injuries in food service workers: a cluster randomized trial. *Scandinavian Journal of Work, Environment & Health*(2), 194–202. 10.5271/sjweh.3790
- Beschorner KE, Albert DL, Chambers AJ, & Redfern MS (2014). Fluid pressures at the shoe-floor-contaminant interface during slips: effects of tread and implications on slip severity. *Journal of biomechanics*, 47(2), 458–463. 10.1016/j.jbiomech.2013.10.046 [PubMed: 24267270]
- Beschorner KE, Albert DL, & Redfern MS (2016). Required coefficient of friction during level walking is predictive of slipping. *Gait & posture*, 48, 256–260. [PubMed: 27367937]
- Beschorner KE, Iraqi A, Redfern MS, Cham R, & Li Y (2019). Predicting slips based on the STM 603 whole-footwear tribometer under different coefficient of friction testing conditions. *Ergonomics*, 62(5), 668–681. 10.1080/00140139.2019.1567828 [PubMed: 30638144]
- Beschorner KE, Siegel JL, Hemler SL, Sundaram VH, Chanda A, Iraqi A, Haight JM, & Redfern MS (2020). An observational ergonomic tool for assessing the worn condition of slip-resistant shoes. *Applied Ergonomics*, 88, 103140. [PubMed: 32678768]
- Cazzaniga S (2021, November 15, 2006). Select ROI in image using spline. MATLAB Central File Exchange <https://www.mathworks.com/matlabcentral/fileexchange/12530-select-roi-in-image-using-spline>
- Cham R, & Redfern MS (2002). Heel contact dynamics during slip events on level and inclined surfaces. *Safety science*, 40(7–8), 559–576.
- Chang W-R, Chang C-C, & Matz S (2011). The Effect of Transverse Shear Force on the Required Coefficient of Friction for Level Walking. *Human Factors*, 53(5), 461–473. 10.1177/0018720811414885 [PubMed: 22046720]
- Grönqvist R (1995). Mechanisms of friction and assessment of slip resistance of new and used footwear soles on contaminated floors. *Ergonomics*, 28, 224–241.
- Hale J, Lewis R, & Carré MJ (2021). Effect of simulated tennis steps and slides on tread element friction and wear. *Sports Engineering*, 24(1), 5. 10.1007/s12283-021-00343-4
- Hanson JP, Redfern MS, & Mazumdar M (1999). Predicting slips and falls considering required and available friction. *Ergonomics*, 42(12), 1619–1633. 10.1080/001401399184712 [PubMed: 10643404]
- Heeluxe Inc. (2021). The Time Machine Shoe Durability Test Is HERE! Heeluxe, Inc Retrieved 7/15/2022 from <https://www.heeluxe.com/the-time-machine-shoe-durability-test-is-here/>
- Hemler SL, Charbonneau DN, Iraqi A, Redfern MS, Haight JM, Moyer BE, & Beschorner KE (2019). Changes in under-shoe traction and fluid drainage for progressively worn shoe tread. *Appl Ergon*, 80, 35–42. 10.1016/j.apergo.2019.04.014 [PubMed: 31280808]
- Hemler SL, Pliner EM, Redfern MS, Haight JM, & Beschorner KE (2020). Traction performance across the life of slip-resistant footwear: preliminary results from a longitudinal study. *Journal of Safety Research*, 74, 219–225. [PubMed: 32951786]
- Hemler SL, Pliner EM, Redfern MS, Haight JM, & Beschorner KE (2022). Effects of natural shoe wear on traction performance: a longitudinal study. *Footwear Science*, 14(1), 1–12.



- Hemler SL, Sider JR, Redfern MS, & Beschoner KE (2021). Gait kinetics impact shoe tread wear rate. *Gait & posture*, 86, 157–161. [PubMed: 33735824]
- Iraqi A, Vidic NS, Redfern MS, & Beschoner KE (2020). Prediction of coefficient of friction based on footwear outsole features. *Applied Ergonomics*, 82, 102963. [PubMed: 31580996]
- Jakobsen L, Lysdal FG, Bagehorn T, Kersting UG, & Sivebaek IM (2022). Evaluation of an actuated force plate-based robotic test setup to assess the slip resistance of footwear. *International Journal of Industrial Ergonomics*, 88, 103253.
- Mars W, & Fatemi A (2002). A literature survey on fatigue analysis approaches for rubber. *International Journal of fatigue*, 24(9), 949–961.
- Moghaddam SRM, Hemler SL, Redfern MS, Jacobs TD, & Beschoner KE (2019). Computational model of shoe wear progression: Comparison with experimental results. *Wear*, 422, 235–241. [PubMed: 37200982]
- Moore DF (1972). *The friction and lubrication of elastomers*, International series of monographs on material science and technology. oxford: pergamon press.
- National Institute for Occupational Safety and Health. (2020, September 11, 2020). Traumatic Occupational Injuries: Fast Facts Centers for Disease Control and Prevention <https://www.cdc.gov/niosh/injury/fastfacts.html>
- Needham JA, & Sharp JS (2016). Watch your step! A frustrated total internal reflection approach to forensic footwear imaging. *Scientific Reports*, 6, 21290–21290. 10.1038/srep21290 [PubMed: 26880687]
- Perkins PJ (1978). Measurement of slip between the shoe and ground during walking (Walkway Surfaces: Measurement of Slip Resistance. ASTM 649.
- SATRA Technology. (2022). SATRA STM 528 Pedatron. SATRA. Retrieved 7/15/2022 from [https://www.satra.com/test\\_equipment/machine.php?id=16](https://www.satra.com/test_equipment/machine.php?id=16)
- Sundaram VH, Hemler SL, Chanda A, Haight JM, Redfern MS, & Beschoner KE (2020). Worn region size of shoe outsole impacts human slips: Testing a mechanistic model. *Journal of biomechanics*, 105, 109797. 10.1016/j.jbiomech.2020.109797 [PubMed: 32423543]
- U.S. Department of Labor- Bureau of Labor Statistics. (2020a). Nonfatal Cases Involving Days Away from Work: Selected Characteristics (2011 Forward) Series ID: CSU00X00000063000
- U.S. Department of Labor- Bureau of Labor Statistics. (2020b). Nonfatal Cases Involving Days Away from Work: Selected Characteristics (2011 Forward) Series ID: CSUE4X00000063000
- Verma SK, Chang WR, Courtney TK, Lombardi DA, Huang Y-H, Brennan MJ, Mittleman MA, Ware JH, & Perry MJ (2011). A prospective study of floor surface, shoes, floor cleaning and slipping in US limited-service restaurant workers. *Occupational and environmental medicine*, 68(4), 279–285. [PubMed: 20935283]
- Verma SK, Zhao Z, Courtney TK, Chang W-R, Lombardi DA, Huang Y-H, Brennan MJ, & Perry MJ (2014). Duration of slip-resistant shoe usage and the rate of slipping in limited-service restaurants: results from a prospective and crossover study. *Ergonomics*, 57(12), 1919–1926. 10.1080/00140139.2014.952348 [PubMed: 25205136]
- Wilson M (1990). Development of Satra Slip Test and Tread Pattern Design Guidelines. *Slips, Trips, and Falls: Pedestrian Footwear and Surfaces*, ASTM STP 1103, 113–123.

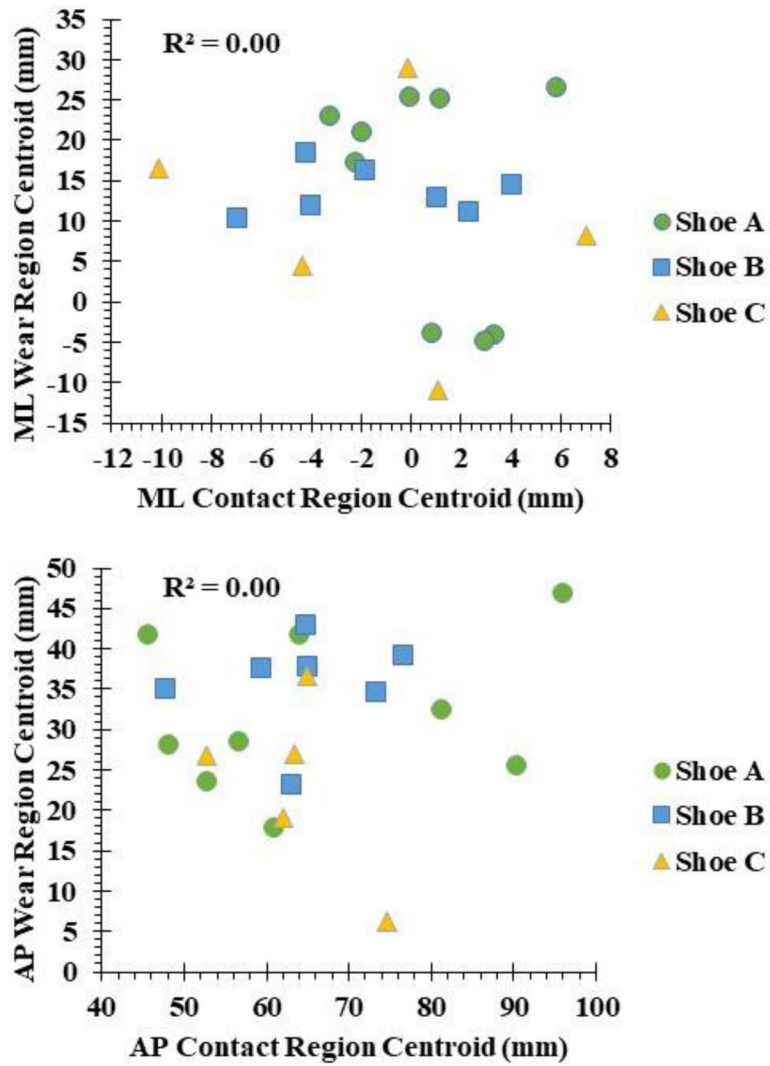
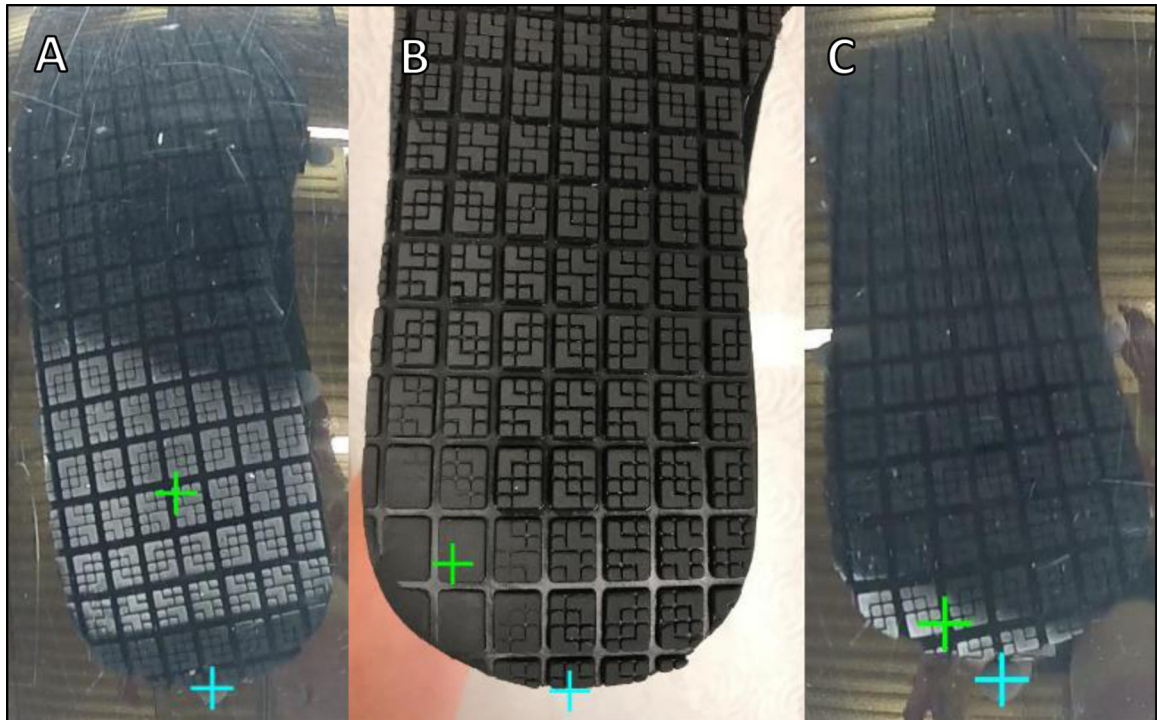
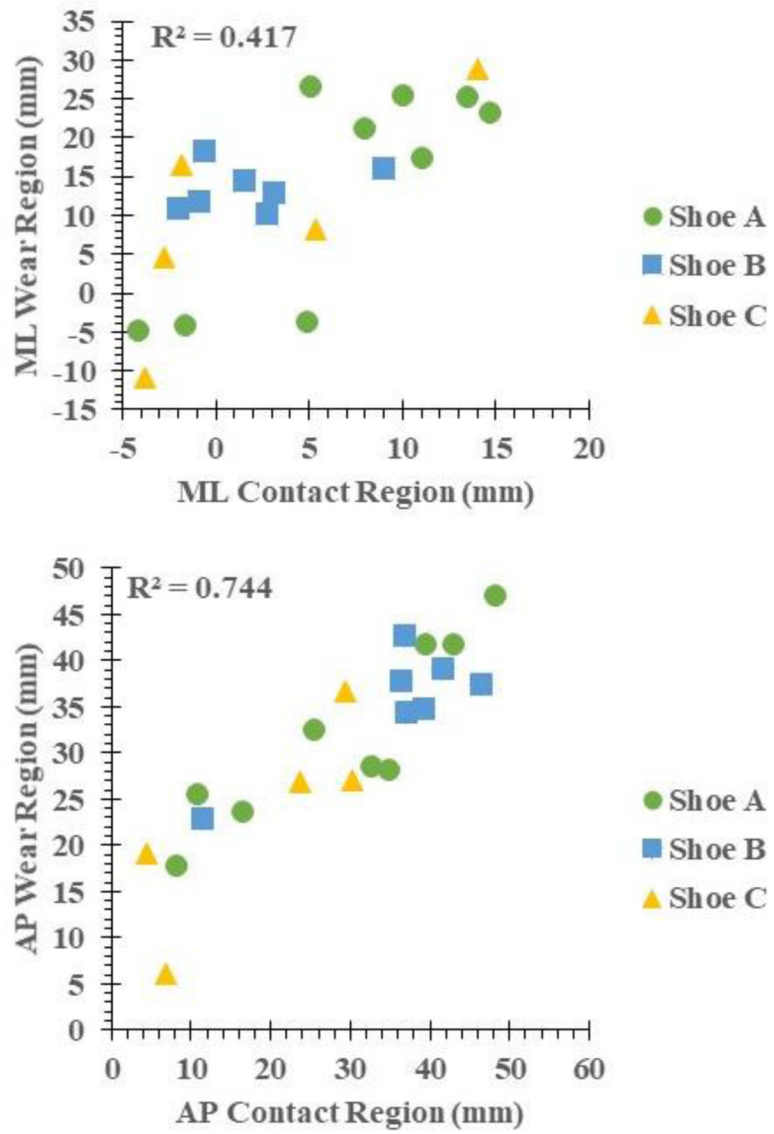


Figure 1: Correlation of centroid coordinates of wear region and contact region at RCOF along medial-lateral (top) and anterior-posterior axes (bottom).



**Figure 2:**

Sample images of a participant's shoe. A) contact region at RCOF. B) worn region after 10 months. C) contact region 17 ms after heel contact. The blue cross indicates the reference point at the bottom edge of the heel, and the green cross indicates the region (contact or wear) centroid.



**Figure 3:** Correlation of centroid coordinates of wear region and contact region at selected timepoints along medial-lateral (top) and anterior-posterior axes (bottom).

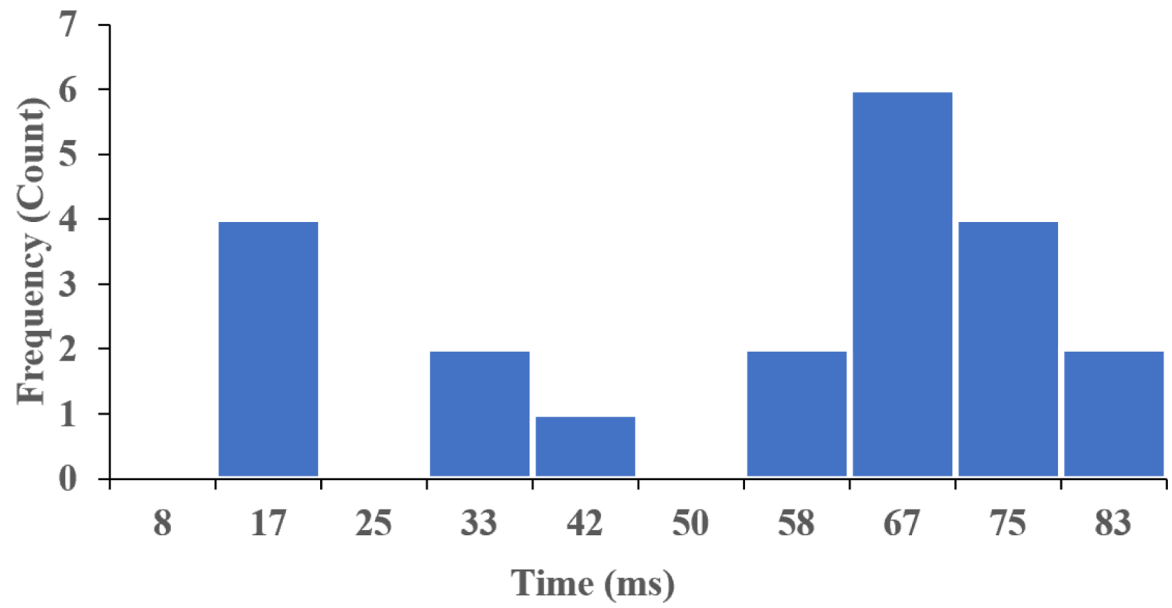


**Figure 4:** Histogram of contact time where the contact region centroid was closest in distance to the wear region centroid. Time points correspond to the frame obtained from the 120 fps camera (Frame 1 = 8 ms, Frame 2 = 17 ms, etc.).






**Figure 5:** Stacked column plot showing proportions of treads that were in contact with the ground and were worn (middle bar, “Both Tread”), not in contact but were worn (top bar, “Worn-only Tread”), and in contact but were not worn (bottom bar, “Contact-only tread”). Data values indicate mean value across participants within shoe type, and error bars indicate standard deviation.



**Table 1:**

Shoe design, brand, and tread parameters for the shoes in this study.

Shoe Code	Shoe/Boot	Brand	Shape and dimensions of characteristic tread (mm)	Tread Depth (mm)	Hardness (Shore A)	Heel Height (mm)*
A	Shoe	SRMax		2.8	48.3	0
B	Shoe	safeTstep		2.7	65.4	0
C	Boot	ShoesForCrews		3.4	49.9	19

\* Measured with the shoe placed on a flat floor surface from the floor to the location where the raised heel meets the rest of the outsole. A value of 0 indicates that there was not a raised heel.